Unbinding force of chemical bonds and tensile strength in strong crystals

Xiaoju Guo[1], **Li-Min Wang**[1], **Bo Xu**[1], **Zhongyuan Liu**[1], **Dongli Yu**[1], **Julong He**[1], **Hui-Tian Wang**[2] and **Yongjun Tian**[1,3]

[1] State Key Laboratory of Metastable Materials Science and Technology, Yanshan University, Qinhuangdao 066004, People's Republic of China
[2] Nanjing National Laboratory of Microstructures and Department of Physics, Nanjing University, Nanjing 210093, People's Republic of China

E-mail: fhcl@ysu.edu.cn

Abstract

A model of covalent and ionic bond strength is proposed in terms of the tensile unbinding force by introducing the concept of the effectively bonded valence electron (EBVE) number of a chemical bond. Bond strength proves to be exclusively dependent on two microscopic parameters: bond length and EBVE number. This model allows us to determine bond strength for a variety of crystals and accounts for the observation that a low-coordination number of binding atoms has a tendency to higher bond strength. For crystals of simple structures, we propose linking bond strength to the theoretical tensile strength of a crystal; the latter reproduces the results of first-principles calculations. The model also allows for the assessment of the theoretical tensile strength of graphene and single-walled nanotubes constructed with typical material systems.

(Some figures in this article are in colour only in the electronic version)

1. Introduction

The relationship between bond strength and the electronic structure of covalent and ionic crystals is a subject of great interest in basic condensed matter physics, chemistry, and materials science. These crystals exhibit excellent functional properties in mechanics, calorifics, electrics, and optics, making them relevant for technical applications. The mechanical properties of the crystals—such as strength and hardness—depend on bond strength [1–3] and other physical quantities, such as potential barriers of a solid state reaction and critical pressure of a solid state phase transition from the low-density phase to the high-density phase, also should relate directly to bond strength.

In solids, however, describing bond strength quantitatively at the microscopic level has proven difficult, and one of the main unsolved problems is to find what microscopic parameters determine bond strength. Fortunately, many covalent and ionic crystals are stable in the same structure, and this makes them suitable for systematic studies of the relationship between bond strength and electronic structure.

Bond strength represents the degree to which each atom linked to a central atom contributes to the valency of the central atom and can be characterized by different scales. Experimentally, bond strength can be indirectly expressed by bond stiffness [4], or quantified by bond energy or bond dissociation energy for a simple molecule and by lattice energy for an ionic crystal [5]. Recently, atomic force microscopy has been applied for the direct measurement of weak noncovalent interaction forces of protein in the piconewton range [6, 7]. Theoretically, the bond strength of an ideal crystal depends on such intrinsic characteristics of chemical bonds as bond length, valence electrons, and the coordination number of two bonding atoms. Pauling defined bond strength s as $s = +z/N$ for a coordination MX_N polyhedron in a complex ionic crystal, where $+z$ is the ionic valence of the M cation and N is the number of coordinating X anions [8]. Brown *et al* found that bond strength s can be modeled with the power-law expression $s = (d_0/d)^{-n}$ for a wide variety of oxide materials, where d_0 and n are two regression constants, and d is the bond length [9]. Recently, Gibbs *et al* provided a more accurate power-law expression: $s = 4.467rd^{-1/0.22}$ for these oxides, where r is the row number of the M cation [10]. They also found that bond
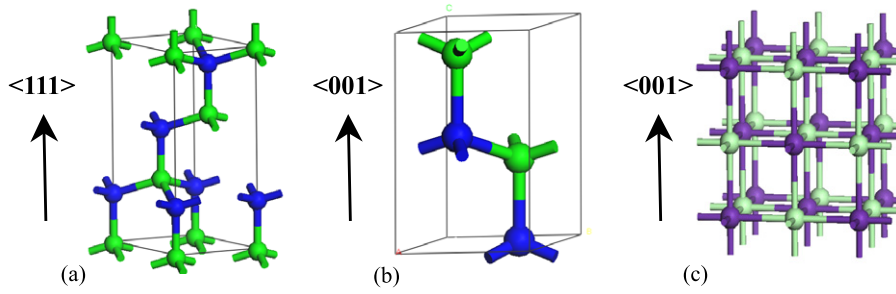
Figure 1. Three typical crystal structures with chemical bonds parallel to tensile directions along $\langle 111 \rangle$ of zincblende (a), $\langle 001 \rangle$ of wurtzite (b), and $\langle 001 \rangle$ of rock salt (c).

strength is related in some way to the value of the electron-density distribution on the bond and that the greater the bond strength, the greater the number of bonding electrons [10].

These definitions and scales of bond strength are valid only for special types of crystals. Establishing a generalized model of bond strength has remained an open challenge. If we can define bond strength with an unbinding force of the chemical bond, the physical figure of bond strength for solids becomes more apparent and more accessible than Pauling's definition or the above-mentioned energy scales. In this paper, we present a simple, semi-quantitative solution to this problem and offer a quantitative determination of the tensile unbinding force of a chemical bond in the entire range (IV–IV, III–V, II–VI, and I–VII) of crystals, in which the sum of the outer shell electrons of the two binding atoms equals 8. This basic principle can be applied also to the estimation of bond strength in such complex crystals as β-Si_3N_4, where the sum of the outer shell electrons of Si and N atoms goes over 8.

2. Model

For any type of chemical bond i–j containing eight valence electrons per atom pair and the coordination numbers of N_i and N_j of atoms i and j, the nominal valence numbers n_i and n_j of two atoms distributed to the i–j bond equal Z_i/N_i and Z_j/N_j, respectively, where Z_i is the valence electron number of atom i. In fact, the bonded electrons localized in the binding region are basically smaller than n_i or n_j. In first-principles calculations, the Mulliken overlap population of a bond provides a measurement of the bonded electrons [11]. For example, the calculated population is 0.75 for C–C bonds in diamond and 0.19 for Na–Cl bonds in NaCl crystal. The greater localization of electron density in the binding region of a bond results in a stronger bond. While the determination of population largely depends on calculation formalisms [12], it is anticipated to find an alternative parameter, which can be easily determined, to serve as the population. We propose to define the effectively bonded valence electron (EBVE) number n_{ij} of i–j bond in terms of the expression,

$$n_{ij} = \frac{n_i n_j}{\sqrt{n_i^2 + n_j^2}}. \qquad (1)$$

The EBVE numbers of various covalent and ionic crystals are listed in table 1, and from the results of diamond and NaCl,

one can see that the EBVE values are comparable with the calculated population.

The ideal tensile strength of an i–j bond can be defined as a maximum tensile force unbinding the i–j bond. Previous studies have highlighted the role of the bond length and valence electrons on the strength of a chemical bond, the power behaviors of the bond length on bond strength is shown [10, 13], and the exponential dependence of the population-related ionicity on the resistance of a bond to indenter is emphasized [1–3, 14]. Therefore, to describe quantitatively the effects of n_{ij} and bond length d_{ij} on bond strength, the tensile unbinding force F_{ij}, is assumed to follow the formalism,

$$F_{ij} = C d_{ij}^{-m} \exp(k n_{ij}), \qquad (2)$$

where C is a proportionality coefficient, and m and k are two different constants.

With the unbinding force of a bond, the ideal tensile strength of a crystal is expected to be accessible. The ideal tensile strength of a crystal has been accurately determined by first-principles calculations [15]. In this work, first-principles calculations were performed by the CASTEP code. Norm-conserving pseudopotentials were used and the exchange–correlation terms were considered by the local density approximation method. The plane-wave cutoff energy was 770 eV, and the Brillouin zone sampling was determined to keep the separation between neighboring k points 0.04 Å^{-1}. The tensile strength calculation was done with the program: the internal coordinates are relaxed for each strain, and then the stress is obtained. For a simple structural crystal, as shown in figure 1, generally, the weakest tensile directions, such as $\langle 111 \rangle$ of the zincblende (ZB) structure, $\langle 001 \rangle$ of wurtzite (WZ), and $\langle 001 \rangle$ of rock salt (RS) are parallel to the axes of broken bonds. Thus, the ideal tensile strength σ_{hkl} of a crystal along the weakest $\langle hkl \rangle$ direction should be correlated with F_{ij} as

$$\sigma_{hkl} = S_{hkl} F_{ij} = C S_{hkl} d_{ij}^{-m} \exp(k n_{ij}), \qquad (3)$$

where S_{hkl}, in units of m^{-2}, is the number of the broken bonds per unit area on the (hkl) plane, which has the lowest bond density. We optimize the three unknown parameters in equation (3) from data in table 1 by using the Levenberg–Marquardt method [16], and obtain the following expressions

$$\sigma_{hkl}^{\text{theor}}(\text{Pa}) = 6.6 \times 10^{-10} S_{hkl} d_{ij}^{-1.32} \exp(3.7 n_{ij}), \qquad (4)$$

Table 1. Parameters related to the bond strength calculations of typical covalent, polar covalent and ionic crystals. a and c are cell parameters, S_{hkl} is the number of the broken bonds per unit area on the (hkl) plane, d_{ij} is the bond length of the $i-j$ bond, and n_{ij} is the effectively bonded valence electron number. σ_{hkl} and $\sigma_{hkl}^{\text{theor}}$ are the ideal tensile strength and the calculated theoretical tensile strength of a crystal in the given direction, respectively. F_{ij}^{theor} is the tensile force unbinding the $i-j$ bond.

Bond (crystal)	Structure $\langle hkl \rangle$	a^{a} (Å)	c^{a} (Å)	S_{hkl} ($\times 10^{20}$ m^{-2})	d_{ij} (Å)	n_{ij}	σ_{hkl}^{b} (GPa)	$\sigma_{hkl}^{\text{theor}}$ (GPa)	F_{ij}^{theor} (nN)
C–C (Dia.)	ZB$\langle 111 \rangle$	3.567	—	0.182	1.545	0.707	93.0[c]	92.4	5.09
Si–Si (ZB-Si)	ZB$\langle 111 \rangle$	5.431	—	0.078	2.352	0.707	21.3	22.9	2.92
Ge–Ge (Ge)	ZB$\langle 111 \rangle$	5.658	—	0.072	2.450	0.707	17.8	20.0	2.77
Sn–Sn (α-Sn)	ZB$\langle 111 \rangle$	6.491	—	0.055	2.811	0.707	10.5	12.7	2.31
Si–C (β-SiC)	ZB$\langle 111 \rangle$	4.348	—	0.122	1.883	0.707	50.1	47.9	3.92
B–N (c-BN)	ZB$\langle 111 \rangle$	3.615	—	0.177	1.565	0.643	66.0[c]	69.7	3.95
Al–P (AlP)	ZB$\langle 111 \rangle$	5.420	—	0.078	2.347	0.643	18.7	18.2	2.31
Ga–P (GaP)	ZB$\langle 111 \rangle$	5.450	—	0.078	2.360	0.643	17.7	17.8	2.29
B–As (BAs)	ZB$\langle 111 \rangle$	4.777	—	0.101	2.069	0.643	30.3	27.6	2.73
Al–As (AlAs)	ZB$\langle 111 \rangle$	5.662	—	0.072	2.452	0.643	16.1	15.7	2.18
Ga–As (GaAs)	ZB$\langle 111 \rangle$	5.653	—	0.072	2.449	0.643	14.6	15.8	2.19
C–C (Lons.)	WZ$\langle 001 \rangle$	2.522	4.119	0.182	1.545	0.707	93.5	92.4	5.09
Si–Si (WZ–Si)	WZ$\langle 001 \rangle$	3.792	6.256	0.080	2.346	0.707	21.3	23.5	2.93
Al–N (AlN)	WZ$\langle 001 \rangle$	3.111	4.978	0.119	1.917	0.643	38.0[d]	36.0	3.02
Ga–N (GaN)	WZ$\langle 001 \rangle$	3.190	5.189	0.116	1.956	0.643	36.3	33.4	2.94
Zn–O (ZnO)	WZ$\langle 001 \rangle$	3.249	5.205	0.109	1.992	0.474	16.7	16.8	1.54
Na–Cl (NaCl)	RS$\langle 001 \rangle$	5.639	—	0.126	2.820	0.165	3.8	3.9	0.31
K–Cl (KCl)	RS$\langle 001 \rangle$	6.292	—	0.101	3.146	0.165	3.2	2.7	0.27
Na–F (NaF)	RS$\langle 001 \rangle$	4.614	—	0.188	2.307	0.165	7.2	7.6	0.40
Na–Br (NaBr)	RS$\langle 001 \rangle$	5.962	—	0.113	2.981	0.165	3.1	3.2	0.29
Na–I (NaI)	RS$\langle 001 \rangle$	6.479	—	0.095	3.240	0.165	2.4	2.5	0.26
Rb–Cl (RbCl)	RS$\langle 001 \rangle$	6.535	—	0.094	3.268	0.165	2.8	2.4	0.25
Mg–O (MgO)	RS$\langle 001 \rangle$	4.217	—	0.225	2.109	0.316	16.8	17.9	0.79
Mg–S (MgS)	RS$\langle 001 \rangle$	5.202	—	0.148	2.601	0.316	9.1	8.9	0.60
Ca–O (CaO)	RS$\langle 001 \rangle$	4.811	—	0.173	2.406	0.316	13.5	11.5	0.67
Ba–O (BaO)	RS$\langle 001 \rangle$	5.539	—	0.130	2.770	0.316	8.5	7.2	0.55

[a] Experimental data taken from the international center for diffraction data (ICDD) cards.

[b] Unless noted, all data of ideal strength are from present first-principles calculations using a method described in [15].

[c] Reference [17].

[d] Reference [18].

and

$$F_{ij}^{\text{theor}}(N) = 6.6 \times 10^{-10} d_{ij}^{-1.32} \exp(3.7 n_{ij}). \quad (5)$$

The square of the correlation coefficient $R^2 = 0.996$ with the mean absolute fractional deviation of $\sim 7\%$ indicates that equations (4) and (5) are accurate enough to estimate σ_{hkl} and F_{ij}.

3. Results and discussion

We have examined a wide variety of covalent and ionic crystals with a single type of chemical bond, for which n_{ij}, d_{ij} and S_{hkl} are already known or can be calculated from the experimental values of the lattice parameters. Using the data in table 1, we obtain a remarkable linear relationship between logarithmic σ_{hkl} and $S_{hkl} d_{ij}^{-1.32} \exp(3.7 n_{ij})$ as shown in figure 2. An optimized C value makes a valid estimate of σ_{hkl} for a broad range of crystals, which have ZB, WZ, and RS structures and pure covalent, polar covalent, and ionic features. For each crystal in table 1, the difference between the present theoretical tensile strength $\sigma_{hkl}^{\text{theor}}$ and ideal tensile strength σ_{ideal} is within the tolerance of ideal strength from first-principles calculations. Reasonably, the simple relationship of F_{ij}^{theor} or

$\sigma_{hkl}^{\text{theor}}$ with d_{ij} and n_{ij} should be semi-quantitatively valid for such a variety of covalent and ionic crystals. Thus, the bond strength of complex crystals such as β-Si$_3$N$_4$, β-C$_3$N$_4$, α-quartz, cubic-gauche (cg)-N and α-Al$_2$O$_3$ can be also predicted using this model. The formed chemical bonds in these crystals are typical two-electron bonds. The former four crystals in the structure obey the 8-N rule. There is a non-bonding electron pair on each N atom for β-Si$_3$N$_4$, β-C$_3$N$_4$, and cg-N and two non-bonding electron pairs on each O atom for α-quartz. Thus n_i and n_j are equal to 1. In α-Al$_2$O$_3$, six O atoms surround each Al atom, and four Al atoms surround each O atom. Therefore, n_{Al} and n_O are 0.5 and 1.5. Table 2 lists the F_{ij}^{theor} values for the individual chemical bond of the five crystals. Obviously, both N–N bond in cg-N and C–N bond in β-C$_3$N$_4$ are stronger than the sp^3-hybridized C–C bond in diamond or lonsdaleite. For a number of covalent, polar covalent, and ionic bonds in the crystals listed in tables 1 and 2, we show the bond strength F_{ij}^{theor} versus bond length d_{ij} in figure 3. Of these 29 kinds of bonds, the strongest bond is N–N, followed by C–N, C–C, Si–O, Si–N, B–N, and Si–C, in sequence. For the bonds in figure 3, all the values of the tensile unbinding forces are located on five lines marked with different n_{ij}, and the bonds with the same n_{ij} locate on the
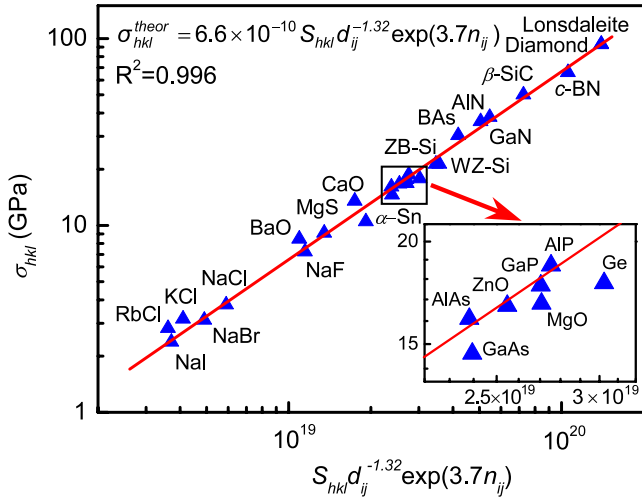
Figure 2. Ideal tensile strength σ_{hkl} of a crystal along the weakest $\langle hkl \rangle$ direction as a function of $S_{hkl}d_{ij}^{-1.32}\exp(3.7n_{ij})$. S_{hkl} is the number of the broken bonds per unit area on the (hkl) plane, d_{ij} the bond length in angstroms, and n_{ij} the effectively bonded valence electron number. The term, $d_{ij}^{-1.32}\exp(3.7n_{ij})$, scales with the maximum tensile force unbinding the $i-j$ bond, F_{ij}. The solid line is from equation (4). The data cover various crystals involving pure covalent crystals (Diamond, Lonsdaleite, ZB–Si, WZ–Si, α-Sn, and Ge), polar covalent solids (c-BN, β-SiN, AlN, GaN, BAs, AlP, GaP, ZnO, AlAs, GaAs and MgS), and ionic solids (CaO, BaO, NaF, NaBr, KCl, RbCl, and NaI).

Table 2. Parameters related to the bond strength calculations of five complex crystals. a and c are cell parameters, d_{ij} is bond length , n_i and n_j are the nominal valence numbers of atom i or j, n_{ij} is effectively bonded valence electron number of $i-j$ bond, and F_{ij}^{theor} is the tensile force unbinding the $i-j$ bond.

Crystal	Bond	a (Å)	c (Å)	d_{ij} (Å)	n_i	n_j	n_{ij}	F_{ij}^{theor} (nN)
β-Si$_3$N$_4$	Si–N	7.602[a]	2.907[a]	1.732	1	1	0.707	4.38
β-C$_3$N$_4$	C–N	6.403[b]	2.405[b]	1.452	1	1	0.707	5.52
α-quartz	Si–O	4.913[a]	5.405[a]	1.608	1	1	0.707	4.83
cg-N	N–N	3.454[c]	—	1.346	1	1	0.707	6.10
α-Al$_2$O$_3$	Al–O	4.759[a]	12.991[a]	1.913	0.5	1.5	0.474	1.62

[a] Experimental data taken from ICDD cards. [b] Reference [19].
[c] Reference [20].

same line. The average coordination number of two binding atoms on the highest line is 3 for N–N and Si–O bonds, 3.5 for C–N and Si–N bonds, and 4 for C–C, Si–C, Si–Si, Ge–Ge, and Sn–Sn bonds, respectively, while the coordination number on the lowest line is 6. This implies that the low-coordination crystal structure has the tendency of higher bond strength.

The theoretical tensile strength of low-dimensional materials such as graphene and nanotubes are of considerable interest in fundamental and technical aspects [21]. It has been pointed out that the sp^2 hybridized C–C bond in the graphene is the strongest chemical bond [22]. The macroscopically estimated theoretical strength of graphene is 326 GPa using the Frenkel model and 140–170 GPa using the Orowan–Polanyi model [23]. Recent first-principles investigations indicate that the ideal tensile strength of graphene in the zigzag $\langle 10 \rangle$ direction is 110 GPa [24], slightly lower than the experimental
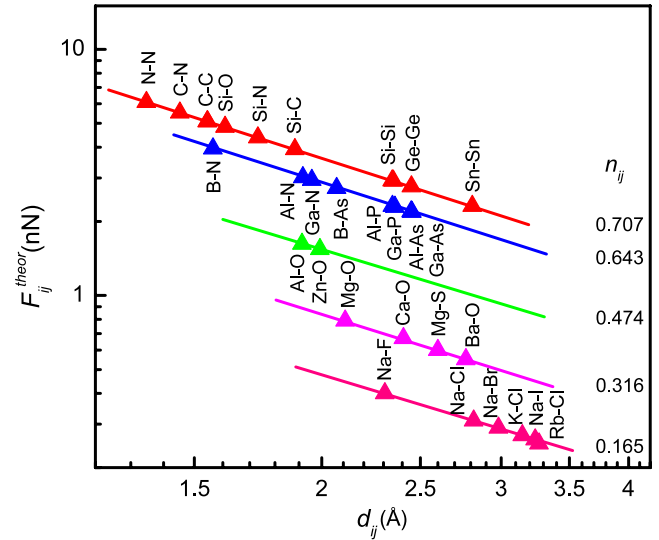

Figure 3. Bond strength F_{ij}^{theor} versus bond length d_{ij} for the chemical bonds in 31 crystals with various values of effectively bonded valence electron number, n_{ij}. The five solid lines are from equation (5).

value of 130 GPa [25]. Here we predict the theoretical tensile strength $\sigma_{10}^{\text{theor}}$ of graphene in $\langle 10 \rangle$ direction using the present model as follows

$$\sigma_{10}^{\text{theor}} = S_{10}F_{cc} = \frac{F_{cc}}{\sqrt{3}d_{cc} \times \delta R}, \qquad (6)$$

where δR is the thickness of graphene taken as the interlayer separation 3.4 Å of graphite [26]. Table 3 lists the values of F_{cc} and d_{cc}. The theoretical tensile strength obtained is 162.7 GPa in the $\langle 10 \rangle$ direction, 20% higher than the experimental value. Similarly, we can predict the theoretical tensile strength $\sigma_{\text{axial}}^{\text{theor}}$ of C, SiC, BN, and AlN single-walled nanotubes (SWNTs) in the axial direction as

$$\sigma_{\text{axial}}^{\text{theor}} = S_{\text{axial}}F_{ij} = \frac{nF_{ij}}{\pi\left[\left(\frac{D_{\text{ep}}+\delta R}{2}\right)^2 - \left(\frac{D_{\text{ep}}-\delta R}{2}\right)^2\right]}, \qquad (7)$$

where D_{ep} is the diameter of the nanotube, and n is the first index of the chiral vector (n, m) for nanotubes. Here we select four zigzag SWNTs of C (10, 0), SiC (10, 0), BN (10, 0), and AlN (10, 0) for our calculations. As table 3 shows, the theoretical tensile strength of C (10, 0) SWNT is 161.0 GPa, almost the same as that of graphene. The first report of the experimental tensile strength of multi-walled carbon nanotube (MWCNT) is only 11–63 GPa [29]. In a recent report, this value reached 150 GPa [23], 93% of our present theoretical value.

Finally, we must address briefly the dependence of the ideal strength on the orientation of the tensile stress. If the stress is not along the axis of a chemical bond, a shear vector component would be generated. If the shear unbinding strength can be also expressed, the ideal strength along a specific direction of a crystal will be accessed. Further studies are therefore expected.

Table 3. Parameters used for the theoretical tensile strength calculations of graphene and nanotubes constructed with five kinds of materials. D_{ep} is the diameter of the nanotubes, d_{ij} is bond length, n_i and n_j are the nominal valence numbers of atom i or j, n_{ij} is the effectively bonded valence electron number of the $i-j$ bond and, F_{ij}^{theor} is the tensile force unbinding the $i-j$ bond. σ_{theor} refers to the calculated tensile strength in the $\langle 10 \rangle$ direction for graphene or along the axial direction for nanotubes. σ_{exp} is the experimental tensile strength.

Bond	Graphene $\langle hk \rangle$/ nanotube (n, m)	D_{ep} (Å)	d_{ij} (Å)	n_i	n_j	n_{ij}	F_{ij}^{theor} (nN)	σ_{theor} (GPa)	σ_{exp} (GPa)
C–C	Graphene $\langle 10 \rangle$	—	1.419[a]	1.333	1.333	0.943	13.6	162.7	130[b]
C–C	C (10, 0)	7.91[c]	1.42	1.333	1.333	0.943	13.6	161.0	11–63[d,e]150[e,f]
Si–C	SiC (10, 0)	9.95[g]	1.80	1.333	1.333	0.943	9.94	93.6	—
B–N	BN (10, 0)	8.11[c]	1.45	1	1.667	0.857	9.65	111.4	—
Al–N	AlN (10, 0)	10.33[h]	1.83	1	1.667	0.857	7.10	64.3	—

[a] Reference [27]. [b] Reference [25]. [c] Reference [28]. [d] Reference [29]. [e] Experimental data of multi-walled carbon nanotubes. [f] Reference [23]. [g] Reference [30]. [h] Reference [31].

4. Conclusions

The above results confirm that bond strength in solids relies strongly on the electronic structure of a solid, in particular, on the EBVE number of the bond. The tensile strength of the C–C bond in graphene and SWCNTs is 2.67 times greater than that in diamonds, and such bonds as Si–C, B–N, and Al–N in the low-dimensional structures of nanotubes also become significantly stronger than C–C bonds in diamond because of higher n_{ij}. The model developed in this study, therefore, proves to be valid for a wide variety of crystals, even for low-dimensional materials such as graphene and nanotubes.

Acknowledgments

References

[1] Gao F, He J, Wu E, Liu S, Yu D, Li D, Zhang S and Tian Y 2003 *Phys. Rev. Lett.* **91** 015502
[2] Simunek A and Vackar J 2006 *Phys. Rev. Lett.* **96** 085501
[3] Li L, Wang X, Zhang F and Xue D 2008 *Phys. Rev. Lett.* **100** 235504
[4] Emmerlich J, Music D, Houben A, Dronskowski R and Schneider J M 2007 *Phys. Rev. B* **76** 224111
[5] Pauling L 1960 *The Nature of the Chemical Bond* (Ithaca, NY: Cornell University Press)
[6] Florin E L, Moy V T and Gaub H E 1994 *Science* **264** 415
[7] Kühner F, Costa L T, Bisch P M, Thalhammer S, Heckl W M and Gaub H E 2004 *Biophys. J.* **87** 2683
[8] Pauling L 1929 *J. Am. Chem. Soc.* **51** 1010
[9] Brown I D and Shannon R D 1973 *Acta Crystallogr.* A **29** 266
[10] Gibbs G V, Rosso K M, Cox D F and Boisen M B 2003 *Phys. Chem. Miner.* **30** 317
[11] Mulliken R S 1955 *J. Chem. Phys.* **23** 1833
[12] Segall M D, Shah R, Pickard C J and Payne M C 1996 *Phys. Rev. B* **54** 16317
[13] Gibbs G V, Hill F C, Boisen M B and Downs R T 1998 *Phys. Chem. Miner.* **25** 585
[14] He J, Wu E, Wang H, Liu R and Tian Y 2005 *Phys. Rev. Lett.* **94** 015504
[15] Roundy D, Krenn C R, Cohen M L and Morris J W 1999 *Phys. Rev. Lett.* **82** 2713
[16] Levenberg K 1944 *Q. Appl. Math.* **2** 164
Marquardt D W 1963 *SIAM J. Appl. Math.* **11** 431
[17] Zhang Y, Sun H and Chen C F 2006 *Phys. Rev. B* **73** 144115
[18] Zhang R F, Sheng S H and Veprek S 2007 *Appl. Phys. Lett.* **91** 031906
[19] He J L, Guo L C, Guo X J, Liu R P, Tian Y J, Wang H T and Gao C X 2006 *Appl. Phys. Lett.* **88** 101906
[20] Eremets M I, Gavriliuk A G, Trojan I A, Dzivenko D A and Boehler R 2004 *Nat. Mater.* **3** 558
[21] Dumitrica T, Hua M and Yakobson B I 2006 *Proc. Natl Acad. Sci. USA* **103** 6105
[22] Coulson C A 1952 *Valence* (Oxford: Oxford University Press)
[23] Demczyk B G, Wang Y M, Cumings J, Hetman M, Han W, Zettl A and Ritchie R O 2002 *Mater. Sci. Eng.* **334** 173
[24] Liu F, Ming P M and Li J 2007 *Phys. Rev. B* **76** 064120
[25] Lee C, Wei X, Kysar J W and Hone J 2008 *Science* **321** 385
[26] Lu J P 1997 *Phys. Rev. Lett.* **79** 1297
[27] Naskin Y and Meyer L 1955 *Phys. Rev.* **100** 544
[28] Hernandez E, Goze C, Bernier P and Rubio A 1998 *Phys. Rev. Lett.* **80** 4502
[29] Yu M Y, Lourie O, Dyer M J, Moloni K, Kelly T F and Ruoff R S 2000 *Science* **287** 637
[30] Zhang Y F and Huang H C 2008 *Comput. Mater. Sci.* **43** 664
[31] Mirzaei M, Seif A and Hadipour N L 2008 *Chem. Phys. Lett.* **461** 246